Analytical and Bioanalytical Chemistry (2022) 414:3729–3739
https://doi.org/10.1007/s00216-022-04020-8

RESEARCH PAPER

Biorecognition of hydrogen peroxide using a novel electrochemical platform designed with *Glossoscolex paulistus* giant hemoglobin

Evair D. Nascimento[1,2] · Vanessa E. Abrantes-Coutinho[3] · Thiago M. B. F. Oliveira[3] · Patrícia S. Santiago[4] · Francisco A. O. Carvalho[2]

Received: 25 January 2022 / Revised: 8 March 2022 / Accepted: 14 March 2022 / Published online: 26 March 2022

Abstract

The giant extracellular hemoglobin of the annelid *Glossoscolex paulistus* (HbGp; 3.6 MDa) is a valuable and underexplored supramolecular hemoprotein system for the biorecognition of reactive oxygen species. In this work, an efficient and simple electrochemical platform was designed for analyzing H_2O_2, using HbGp covalently immobilized on Nafion®-modified glassy carbon electrode, named as HbGp/Nafion/GCE. Voltammetric and spectroscopic studies revealed the importance of prior modification of the electrodic support with the conducting polymer to obtain satisfactory hemoglobin electroactivity, as well as a biocompatible microenvironment for its immobilization. In terms of biological activity, it was observed a greater reactivity of the biomolecule in acidic medium, enabling the detection of the analyte by a quasi-reversible mechanism, whose kinetics was limited by analyte diffusion. In the presence of H_2O_2, the native structure of hemoglobin (oxy-HbGp (Fe^{2+})) oxidizes to ferryl-HbGp (Fe^{4+}) and this redox reaction can be monitored on HbGp/Nafion/GCE with a detection limit of 8.5×10^{-7} mol L^{-1}. In addition to high sensitivity, the electrochemical biosensor also provided reproducible, consistent, and accurate measurements. The electroanalytical method showed an appropriate performance to quantify different levels of H_2O_2 in milk samples, proving the potential of HbGp/Nafion/GCE for this purpose.

Keywords *Glossoscolex paulistus* · Giant hemoglobins · H_2O_2 · Electrochemical biosensors · Electroanalysis

Introduction

Giant extracellular hemoglobins are proteins involved in the respiratory system of annelids and molluscs [1, 2], being characterized by cooperativity and affinity to bind oxygen comparable to mammalian hemoglobins. Other peculiar oligomeric characteristics, such as those found for *Glossoscolex paulistus* hemoglobin (HbGp), have attracted the attention of many researchers in relation to its biotechnological potential. HbGp has a highly organized native structure, containing 144 polypeptide chains with heme groups (porphyrin sites coordinated to iron atoms) called **a**, **b**, **c**, and **d**, besides 36 polypeptide chains without heme groups, called chains linker $\boldsymbol{L_1}$, $\boldsymbol{L_2}$, and $\boldsymbol{L_3}$ [3–6]. The role of these subunits is probably related to the maintenance of the oligomeric structure [6, 7], whose molecular mass is 3.6 MDa [8]. Figure 1 illustrates the three-dimensional structure of HbGp along with its constituent subunits. The presence of the heme group also makes this macromolecule electroactive [9, 10], as well as vertebrate hemoglobins [11]. Furthermore, this macromolecule has high oligomeric stability and resistance to auto-oxidation under stress conditions caused by changes in pH, temperature, concentration of salts, and denaturing agents [3, 12–17], enabling its application as a robust biorecognition element and/or carrier of reactive oxygen species.

Despite the great technological potential of HbGp, most research is focused on understanding its properties and

✉ Francisco A. O. Carvalho
adriano.carvalho@unifesspa.edu.br

1 Departamento de Química, Universidade Federal de São Carlos, Rod. Washington Luís km 235, São Carlos, SP 13565-905, Brazil

2 Universidade Federal Do Sul E Sudeste Do Pará, Folha 17, Quadra 04, Lote Especial, Marabá, PA 68505-080, Brazil

3 Centro de Ciência E Tecnologia, Universidade Federal Do Cariri, Avenida Tenente Raimundo Rocha, 1639, Cidade Universitária, Juazeiro Do Norte, CE 63048-080, Brazil

4 Universidade Estadual Paulista, Instituto Avançado de Estudos Do Mar, Campus de Registro, Av. Nelson Brihi Badur, 430 - Vila Tupy, Registro, SP 11900-000, Brazil

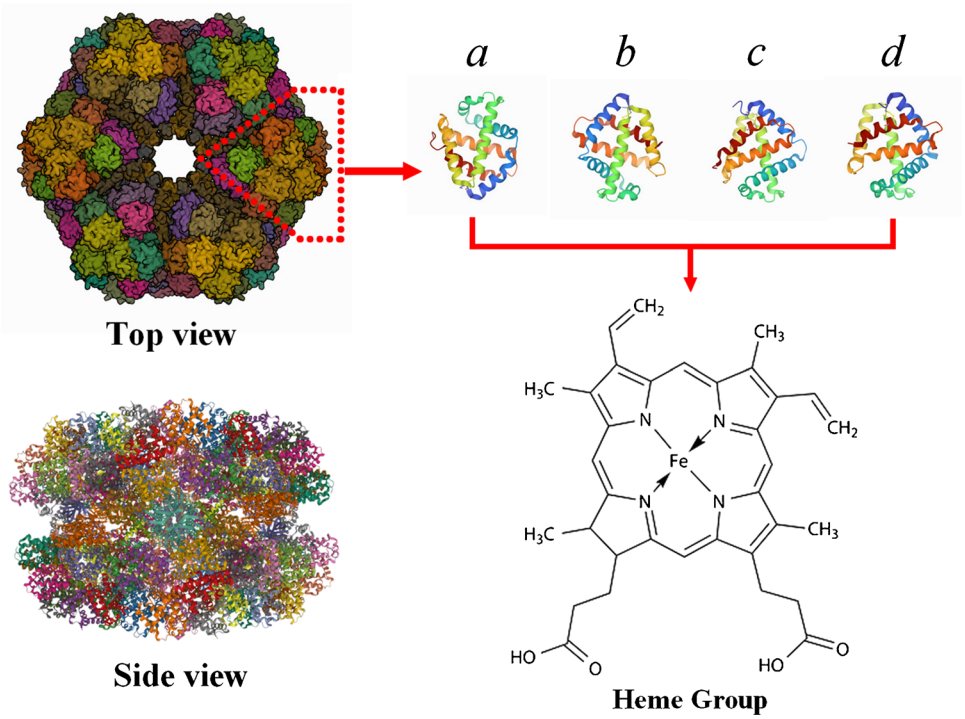

Fig. 1 Crystallographic structure of the giant hemoglobin from *Glossoscolex paulistus,* its subunits, and heme group representation. Adapted from Protein Data Bank (PDB: 4U8U)

mechanisms of action, while its possible applications remain virtually unexplored [18–23]. Carvalho et al. [14], for example, observed by analytical ultracentrifugation and dynamic light scattering data that the oligomeric structure of HbGp remains especially intact at pH 7.0, reaching a hydrodynamic diameter around 28 nm. Caruso et al. [24] reported that it has significant peroxidase activity in the presence of guaiacol and catalyzes the reduction of hydrogen peroxide (H_2O_2). Libardi et al. [25] complemented this research, showing through spectroscopic data that high concentrations of H_2O_2 turn meta-HbGp (Fe^{3+}) into ferryl-HbGp (Fe^{4+}) species, and changes in the oxidation state of iron have important implications for protein activity. These studies also suggest that HbGp, as well as other globins [26–31], combines interesting properties to be adapted in electrochemical biosensors engineered for hydrogen peroxide.

The redox reaction between HbGp and H_2O_2 can be studied, for example, for peroxide biosensing in complex samples. This is important because H_2O_2 is widely used as a preservative in the food industry, especially in dairy products [32, 33], stimulating the endogenous lactoperoxidase antibacterial system [34, 35]. However, this practice can trigger severe side effects, such as gastritis and intestinal inflammation [36], leading to its ban in many countries. Monitoring this oxidizing agent is important, but also challenging because H_2O_2 is extremely reactive and has a short half-life, requiring devices that provide fast, reproducible, specific, and accurate analyses. Alternative enzymatic and non-enzymatic biosensors have been proposed, but depending on the sample handling conditions in terms of pH, temperature, supporting electrolyte, and electroactive interferences, their application may be unfeasible, demanding more robust and versatile devices.

In order to meet these requirements and contribute to new alternatives for monitoring this analyte, a novel electrochemical biosensor for H_2O_2 is proposed here, using HbGp as a biorecognition element. The working device was developed with a glassy carbon electrode modified with Nafion®, which was used as a biocompatible support for the direct immobilization of giant extracellular hemoglobin (HbGp/Nafion/GCE). Typical electroanalytical parameters related to the interaction of the analyte with the biosensor were analyzed and critically discussed to assess the performance of the proposed method. Comments on changes in physicochemical parameters associated with the integrity and activity of the bioelement were also included. HbGp/Nafion/GCE electrochemical biosensor was also tested to monitor low levels of H_2O_2 in bovine milk samples, and the main protocols and results will be highlighted below.

Material and methods

Chemicals

All reagents used were of analytical purity and purchased from Sigma-Aldrich. The H_2O_2 stock solution (1.0×10^{-3} mol L^{-1}) was produced from the dilution of its analytical standard. For biosensor development, Nafion® D-520 with (5% w/w dispersion) was used on GCE to

anchor HbGp (20 mg mL^{-1}). 0.1 mol L^{-1}. Phosphate buffer electrolytic solution ($5.0 \leq pH \leq 9.0$) was prepared by mixing suitable amounts of Na_2HPO_4 and NaH_2PO_4. The pH adjustments were made with NaOH and HCl solutions, both at 0.1 mol L^{-1}. All aqueous solutions were prepared with ultrapure water ($\rho = 18$ MΩ cm^{-1}) from a Millipore Milli-Q system—Brazil.

Protein extraction and purification

Glossoscolex paulistus annelid is prevalent in sites near Piracicaba and Rio Claro cities in the state of São Paulo, Brazil. *G. paulistus* hemoglobin (HbGp), in the oxy-form, was prepared as described in [14, 37]. The final protein concentration in our stock solution was in 20 mg mL^{-1}, in Tris–HCl 100 mmol L^{-1} buffer, pH 7.0. The excess of oxidant was removed by dialysis against the same buffer for 3 h. The concentration was determined spectrophotometrically using the extinction coefficient for oxy-HbGp, ε415 nm = 5.5 ± 0.8 $(mg/mL)^{-1}$ cm^{-1}.

Instrumentation

The electrochemical experiments were performed in a conventional three-electrode cell configured with HbGp/Nafion/GCE biosensor, platinum counter-electrode, and Ag/AgCl (KCl 3.0 mol L^{-1}) reference electrode. The measurements were performed with an Autolab PGSTAT 128 N/FRA32M computer-controlled potentiostat/galvanostat (Metrohm-Autolab; The Netherlands), handled by NOVA 2.0 software. Additional information on hemoglobin stability was studied by UV–visible spectroscopy, using a Cary 50 conc (Varian; Australia) spectrophotometer, either alone or in the presence of Nafion or H_2O_2, ranging the wavelength from 700 to 300 nm. Whenever necessary, pH adjustments were checked by direct potentiometry, using an Orion 5Star multiparameter (Thermo Electron Corporation—USA) equipped with a (H^+)-ion-selective electrode.

Electrochemical procedures

Initially, the performance of HbGp/Nafion/GCE biosensor was evaluated by cyclic voltammetry (CV), ranging the electrochemical potential from − 0.5 V to 1.4 V (vs Ag/AgCl/Cl^-_{sat}), using different scan rates (100–150 mV s^{-1}) and pHs (5.0–9.0). The obtained data were carefully studied to understand the electroactivity, mass- and charge-transport phenomena, mechanism, and kinetics of the H_2O_2 redox reaction at the biosensor/solution interface. Charge-transfer resistance data were obtained by electrochemical impedance spectroscopy (EIS) at open circuit potential, using a frequency range from 10 kHz to 100 MHz with 10 mV of amplitude. Square-wave voltammetry (SWV) was used to quantify H_2O_2 in commercial milk samples, after optimizing the critical parameters that control the electrochemical signal in this technique, i.e., frequency (*f*; 25–250 Hz), amplitude (*a*; 5–60 mV), and potential increment (Δ*Es*; 1–6 mV). Optimization was based on the maximum peak current value (I_p), displacement of peak potential (E_p), and changes of half-peak width ($\Delta E_{p/2}$). All experiments were carried out at room temperature (25 °C), using 0.1 mol L^{-1} phosphate buffer as an electrolyte.

Spectroscopic procedures

UV–visible spectroscopy assays were carried out in order to assess the biocompatibility of Nafion® for the immobilization of hemoglobin. Initially, 100 µL of the conductive polymer was placed in the cuvette and left to rest at room temperature until all solvent had evaporated. After drying, 1.5 mL of 0.2 mg mL^{-1} HbGp solution was added to the cuvette, and spectra were collected after 5 min of hemoglobin-polymer interaction. Subsequently, the amount of free HbGp and its majority form (meta-HbGp or ferryl-HbGp) were estimated by redox titration, using H_2O_2 (1.99×10^{-6} to 9.08×10^{-5} mol L^{-1}) as titrant.

Biosensor production

For biosensor development, GCE was used as support. Its surface was manually cleaned with a polishing cloth (LAM PLAN S.A., France) containing Al_2O_3 suspension (particle size 0.05 µm), followed by an ultrasonic bath for 5 min, and rinsing with distilled water. After this process, the active surface (1.5 mm^2) of the electrode support was covered with 10 µL of Nafion® by drop-coating and kept at room temperature until solvent evaporation. The same process was employed for the direct immobilization of 10 µL of 25 mg mL^{-1} HbGp, producing HbGp/Nafion/GCE working biosensor. Scheme 1 provides a general representation of biosensor development and H_2O_2 detection mechanism.

Evaluation and application of the procedure

Analytical curves were obtained by SWV from peak currents recorded at different concentrations of H_2O_2 (1.99×10^{-6} to 1.57×10^{-5} mol L^{-1}). The coefficients of the resulting linear regression equation were used to calculate the limits of detection (LOD) of the method, according to studies reported in the literature [21]. The precision of the proposed electroanalytical procedure was evaluated by relative standard deviations (RSD%) from consecutive measurements of H_2O_2 (1.18×10^{-5} mol L^{-1}) performed intraday ($n = 8$) and interday ($n = 4$). Reproducibility tests were performed comparing the responses obtained with five different biosensors, which were developed and used

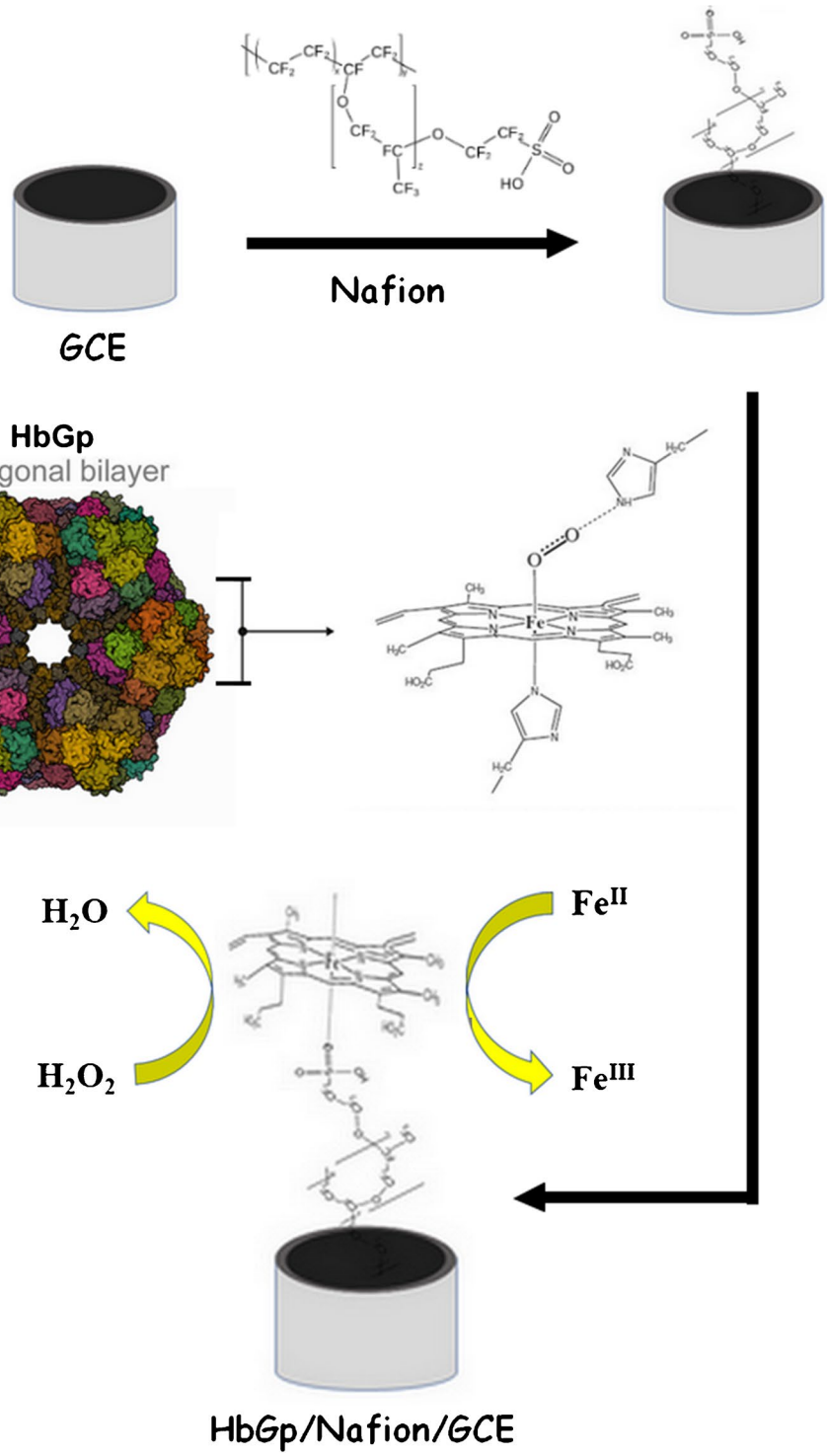

Scheme 1 General representation of HbGp-based biosensor development and H_2O_2 detection mechanism (PDB: 4U8U)

under the same optimized conditions. Thinking about using the procedure to quantify peroxide in bovine milk samples, assays in the presence of lactose, vitamin C, calcium, and magnesium were carried out to evaluate the influence of these substances/ions on the electroanalytical signal. HbGp/Nafion/GCE biosensor was employed to quantify H_2O_2 (3.98×10^{-6} to 1.57×10^{-5} mol L^{-1}) in commercial milk samples, containing a total fat content (11%) and conserved at pH ≈ 6.6 at 5 °C, so that no pre-treatment or sample cleaning steps were required. All measurements were performed in triplicate.

Results and discussions

Electrochemical behavior of HbGp

The electrochemical behavior of HbGp immobilized on GCE and Nafion/GCE was studied by CV at 50 mV s^{-1}, using phosphate buffer (pH = 7.0) as an electrolyte. According to data in Fig. 2A, it can be seen that no redox process is verified when the protein is directly immobilized on bare GCE. This result was associated with a weak interaction between biomolecule and electrode surface, leading to protein dissolution in the presence of the electrolyte. In fact, the low adhesion and detachment of HbGp from the GCE surface were critical and visually noticeable. In addition, some studies proved that iron atoms coordinated to heme groups of globins are not electroactive when directly immobilized on the most common types of surfaces, including carbon ones [38, 39]. The chemical inertness of iron in this case is attributed to the location of the heme groups in the macromolecule, which are immersed inside the oligomeric structure (hydrophobic pocket) and away from the charge-transfer layer [38, 40, 41]. On the other hand, when HbGp was immobilized on Nafion/GCE, well-defined oxidation and reduction processes were observed at 0.91 and 0.20 V (vs Ag/AgCl/Cl^-_{sat}), respectively, which have been associated with changes in the oxidation state of the iron contained in the porphyrin centers. It is evident that this result was favored by Nafion, since its conductive nature reduces the energy gap that delimits the transfer of electrons at the electrode/solution interface [35, 36]. EIS data also showed that the conductive polymer improved charge-transfer resistance, promoting a decrease in the semicircle in Nyquist diagrams (Fig. 2B). A contrary effect was observed after protein immobilization, suggesting good adherence of the biomolecule to the device surface [42].

Following the diagnostic criteria of cyclic voltammetry, the studied redox process is classified as quasi-reversible, corroborating previous studies performed with other hemoglobins [27, 37, 38]. The large peak-to-peak difference between anodic and cathodic waveforms is attributed to the greater stability of oxy-HbGp (reduced form) when compared to meta-HbGp (oxidized form). The oxidation process is more difficult to occur because the heme group involved is located in a predominantly hydrophobic region, limiting molecular solvation [9]. Furthermore, Fig. 2A also shows another low-intensity oxidation process at 0.45 V that precedes the main anodic peak and is probably associated with the oxidation of iron present in subunits less stable under stress, such as the trimeric subunit ***abc***. We found that this process becomes more evident under denaturation conditions, such as in alkaline medium or in high concentrations of hydrogen peroxide. More details about this effect will be presented in the next sections.

The redox process of HbGp on Nafion/GCE changes slowly over consecutive potential scans. After fifty cycles, the anodic and cathodic peak currents decreased by 13.4% and 5.6%, respectively. The anodic peak potential also displaced 60 mV from the initial value, while the cathodic peak potential was almost constant. Even so, the general voltammetric profile of hemoglobin was kept, indicating that

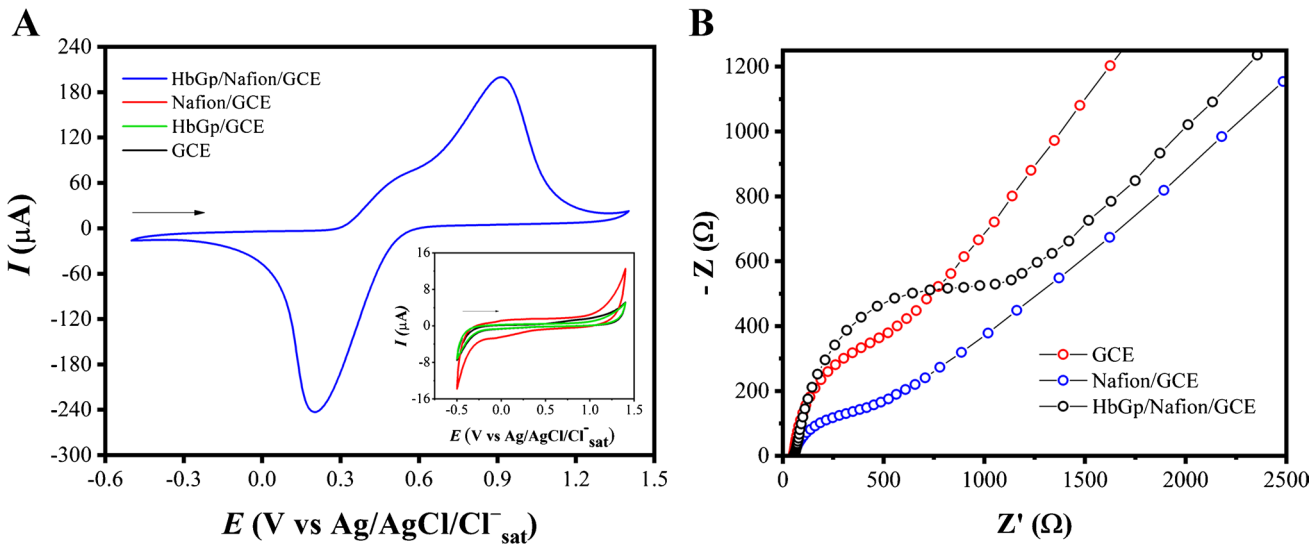

Fig. 2 **A** Cyclic voltammogram recorded with HbGp/Nafion/GCE in phosphate buffer (pH = 7.0), using 50 mV s^{-1}. The results obtained with GCE, HbGp/GCE, and Nafion/GCE are in the figure insert. **B** Nyquist plot recorded at the oxidation peak potential of $[Fe(CN)_6]^{3-}$ (5.0 mmol L^{-1}) in 0.1 mmol L^{-1} H_2SO_4, using a frequency range from 10 kHz to 100 MHz and 10 mV of amplitude

it retains its activity and remains adhered onto the modified electrode (Fig. S1). This behavior is important for the development of electrochemical biosensors, as the stability of the biorecognition element implies reproducibility of the device under study [43]. In other words, any external factor that abruptly disturbs the stability of a biomolecule will promote its denaturation, compromising its functions and possible applications [44].

Typical cyclic voltammograms registered with HbGp/Nafion/GCE in phosphate buffer (pH = 7.0), using different scan rates (v; 10−150 mV s^{-1}), indicated diffusion-limited electrode kinetics. Figure S2A shows that increasing v raises the values of I_p, E_p, and $E_{p/2}$ in a non-linear way, as is usually observed in quasi-reversible processes [45]. Plotting I_{pc} vs. $v^{1/2}$ (Fig. S2B), a relatively linear relationship ($R^2 = 0.9881$) was observed, whose slope reveals an electrodic area of 3.712 ± 0.289 mm^2 [46]. From log I_{pc} vs. log v ($R^2 = 0.9885$; Fig. S3), new evidence of diffusion-controlled mass transport was found [47]; slope = 0.651 ± 0.050. The loss of linearity in this last relationship may be related to charge-transfer phenomena confined in the chemical structure of the biomolecule itself and/or between the different constituent layers of the electrochemical biosensor [48]. As mentioned earlier, high values of v make the voltammetric peaks broader and compromise the method selectivity when the analysis is performed in the presence of interfering agents. The sensitivity of the procedure becomes more expressive at $v \leq 100$ mV s^{-1}, especially when evaluated from the cathodic process; higher I_p values. Hence, this peak was chosen as the electroanalytical signal for the detection of H_2O_2 in further experiments, using $v = 100$ mV s^{-1}.

pH effect

Changes in pH can be critical for the structural conformation of hemoglobins and, consequently, for their biological activity [49–51]. In the case of HbGp, such changes have a drastic effect on the organization of polypeptide chains and primary coordination spheres around the iron centers [52]. Voltammetric data recorded at different pHs (5−9) also proved that the electroactivity of this macromolecule is affected, as shown in Fig. 3. Anodic and cathodic peaks are observed throughout the range studied, but I_p values progressively decrease as the medium becomes alkaline. At the same time, E_p values displaced towards more negative values. At pH > 8, no signal was observed due to dissociation and subsequent denaturation of hemoglobin, making all heme groups more accessible to the solvent. This loss of stability and electroactivity corroborates detailed studies with HbGp conducted by Moreira et al. [53] and Carvalho et al. [14], giving greater credibility to the results obtained. Increased pH leads to loss of oxy-HbGp stability, evidenced by the oxidation of heme iron and its dissociation into smaller

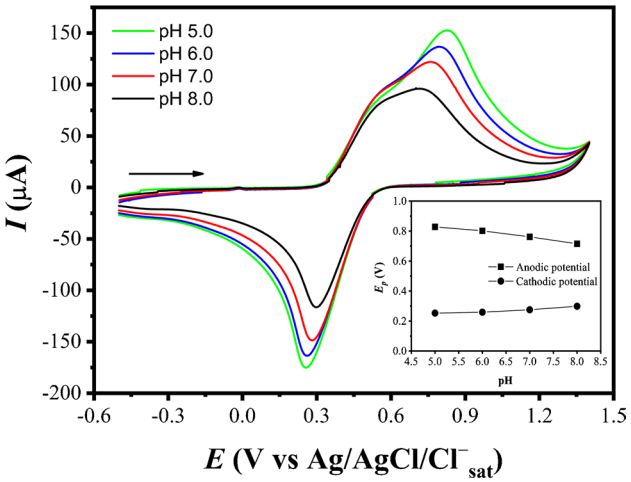

Fig. 3 Cyclic voltammograms recorded with HbGp/Nafion/GCE at 50 mV s^{-1}, using phosphate buffer adjusted to different pHs (5.0–8.0) as electrolyte. Figure inset shows the effect of pH on anodic and cathodic peak potentials

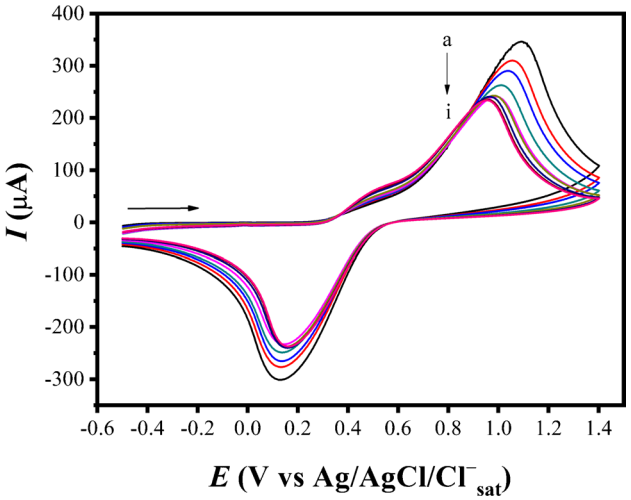

Fig. 4 Cyclic voltammograms recorded with HbGp/Nafion/GCE at 50 mV s^{-1}, using phosphate buffer (pH = 5.0) and different concentrations of H_2O_2 ($a = 1.99$; $b = 3.98$; $c = 5.96$; $d = 7.94$; $e = 11.86$; $f = 15.75$; $g = 19.61$; $h = 25.34$; and $i = 31.01$ μmol L^{-1})

subunits, such as dodecamer (***abcd***)$_3$ and tetramer ***abcd*** [14]. Although the results indicate greater HbGp reactivity under more acidic conditions, adjustment requires attention as it also denatures at pH < 5.

Interaction with H_2O_2

The reaction between H_2O_2 and HbGp is really critical, being able to inhibit the working electrochemical biosensor signal as the concentration of the oxidizing agent increases, as indicated in Fig. 4. This trend continues until 1.57×10^{-5} mol

L^{-1} H_2O_2, remaining practically constant thereafter. This is because the redox reaction with the most exposed iron sites reaches equilibrium, and the reaction kinetics is limited by the diffusion of the analyte towards the more protected sites [54]. Since the resistivity of the system continually changes, the potential values also keep changing, but the currents reach a plateau. The addition of H_2O_2 further reduces peak-to-peak values and increases the reversibility of the redox reaction, which was expected because the dissociation of the oligomeric structure makes the heme groups more accessible to the solvent and susceptible to electrochemical processes.

The bioactivity of HbGp in the presence of Nafion and H_2O_2 in solution was also investigated by UV–visible spectroscopy. Figure 5 shows spectra of the main results obtained under the indicated conditions. In its native state, hemoglobin contains Fe^{2+} ions preserved in its porphyrin domains [24]. It presents an intense Soret band at 414 nm and Q bands (alpha and beta) at 539 nm and 574 nm. The spectrum recorded in the presence of Nafion is practically the same, with only a decrease in the absorbance of the aforementioned bands due to sample dilution, and the appearance of another low-intensity band at 630 nm (insert in Fig. 5). This last sign is characteristic of high-spin species, indicating that small fractions of hemoglobin were partially oxidized in the regions of interaction with the conducting polymer. However, the spectral similarity indicates that HbGp remained mostly in its native form, therefore Nafion offers a biocompatible microenvironment to immobilize this biomolecule. In contrast, H_2O_2 had a much more drastic effect, promoting an expressive reduction of the Soret and Q bands, in addition to their displacement towards the red region of the visible spectrum. The result obtained is strong evidence of the formation of ferryl-HbGp as an oxidation product [25].

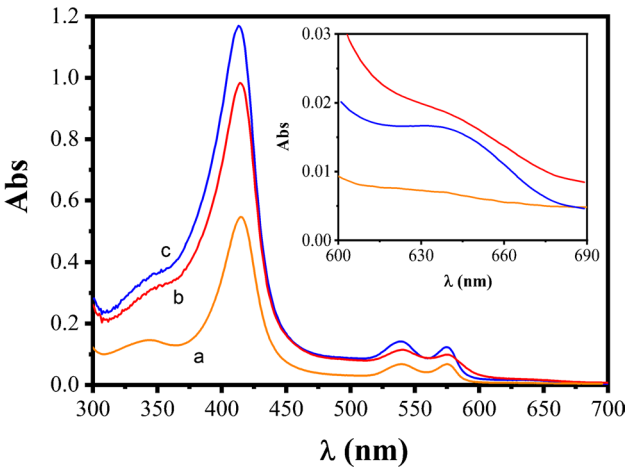

Fig. 5 UV–visible absorption spectrum for (a) pure HbGp and in the presence of (b) Nafion and (c) H_2O_2. The insert highlights the Q-band spectral region in amplified format

Electroanalytical parameters

The ability of HbGp/Nafion/GCE to detect H_2O_2 was explored by SWV, after optimization of critical parameters for signal sensitivity (25–250 Hz frequency, 5–60 mV amplitude, and 1–6 mV potential increment), in order to develop an alternative electroanalytical method for the analyte under study. To obtain greater detection capacity and selectivity, based on the values of I_p, E_p, and $\Delta E_{p/2}$, the best voltammetric parameters were $f = 150$ Hz, $a = 30$ mV, and $\Delta E_s = 2$ mV (Fig. S4; Supplementary Material).

Figure 6 shows the analytical curve used for the determination of H_2O_2 (1.99×10^{-6}–1.57×10^{-5} mol L^{-1}) with HbGp/Nafion/GCE, using phosphate buffer (pH = 5.0) as electrolyte. The high correlation found for the linear adjustment of the data ($R^2 = 0.9949$) proves that the resulting regression equation I_p (μA) = 94.109–3.548 [H_2O_2] (μmol L^{-1}) is representative to describe the data variance. LOD value was 8.5×10^{-7} mol L^{-1} suggesting that the electrochemical biosensor is adequate to quantify the analyte even at low concentrations. As can be seen in Table 1, the sensitivity obtained was equivalent or higher than the other electrochemical methods reported in recent years, compared with enzymatic or non-enzymatic methods. Measurement precision was maintained even when assessed by intraday (RSD = 3.4%; $n = 8$) and interday tests (RSD = 4.7%; $n = 4$). Comparing the response obtained with different devices (RSD = 5.4%; $n = 3$), it was found that the accuracy was not compromised either. Additionally, the signal decay caused by H_2O_2 (1.0×10^{-5} mol L^{-1}) was not significantly influenced when the tests were performed with equimolar

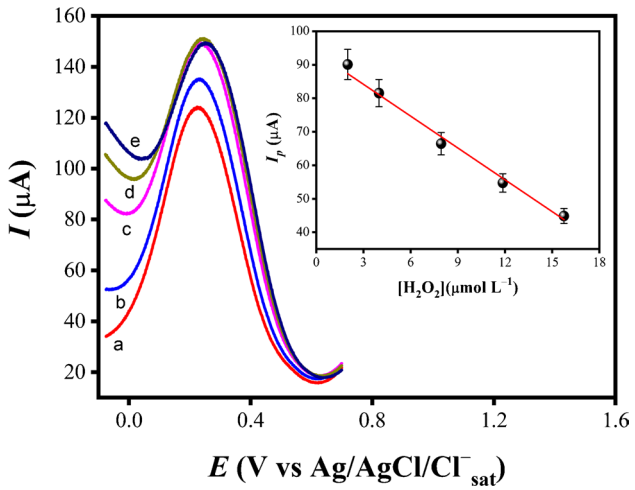

Fig. 6 Square-wave voltammograms obtained for H_2O_2 ($a = 1.99$; $b = 3.98$; $c = 7.94$; $d = 11.86$; and $e = 15.75$ μmol L^{-1}) on HbGp/Nafion/GCE in phosphate buffer (pH = 5.0), using 150 Hz frequency, 30 mV amplitude, and 2 mV potential increment. The insert corresponding analytical curve

Table 1 Comparison of the analytical performance of the HbGp/Nafion/GCE biosensor with enzymatic and non-enzymatic sensors reported in the literature for the determination of H_2O_2

Configuration of electrochemical methods	Linear range (μmol L^{-1})	LOD (μmol L^{-1})	Reference
Hb/NIBA-IL/MWCNT/GCE	10–6300	3.2	[27]
Cyt c/TPP-HA[TFSI]/MWCNT/GCE	20–892	6.2	[29]
Nafion/Hb/Au-TiO_2NSs-rGO/GCE	7.5–250	3.0	[55]
HRP/Ti_3C_2/Nafion/GCE	5.0−8000	1.0	[56]
Hb/PAMAM-AuNPs/GCE	20–950.22	6.1	[57]
Hb/GO/Dy_2O_3/GCE	5–300	2.0	[58]
Nafion/HRP-AuNCs/GCE	10–3270	0.99	[59]
Mb–SGO–Nafion/GCE	10–100	1.5	[60]
Hb-AuNPs@MoS_2/GCE	10–300	4.0	[61]
Fe_3O_4@PANI/rGO/GCE	100−1500	4.45	[62]
Ag-Au/rGO/TiO_2/GCE	10−30,000	3.0	[63]
Fe_2P/NP C/GCE	100−1000	60	[64]
HbGp/Nafion/GCE	1.99–15.74	0.85	In this study

Legends: *Hb* hemoglobin; *GCE* glassy carbon electrode; *NIBA-IL* naphthylimidazolium butyric acid ionic liquid; *MWCNT* multiwalled carbon nanotube; *HRP* horseradish peroxidase; *Au-TiO2NSs- rGO* Au nanoparticles and TiO_2 nanosheets co-modified reduced graphene oxide nanocomposite; *PAMAM* polyamidoamine; *AuNPs* gold nanoparticles; *Cyt c* cytochrome c; *GO* graphene oxide 3; *Dy2O3* dysprosium oxide; *AuNCs* Au nanoclusters; *SGO* sulfonated graphene oxide; *Mb* myoglobin; *MoS2* molybdenum disulfide; *rGO* reduced graphene oxide; *PANI* polyaniline; *Fe_2P/NP C* Fe_2P modified N, P co-doped carbon

amounts of lactose, vitamin C, Ca^{+2}, and Mg^{+2}, which are substances/ions commonly found in bovine milk samples. The analytical performance achieved suggests that HbGp/Nafion/GCE can be quite efficient to quantify H_2O_2 in the above-mentioned matrix.

Application

The efficiency of HbGp/Nafion/GCE to quantify H_2O_2 residues in real milk samples was evaluated. Despite several reports proving the adulteration of commercial samples with different concentrations of the analyte, we did not identify the presence of H_2O_2 in the samples studied. For this reason, the samples were spiked (3.98−15.48 μmol L^{-1}) to assess the applicability of the method. The data in Table 2 show that the recovery values were expressive, ranging from 91.93 to 107.84%. The performance was practically the same, regardless of using raw, centrifuged, or diluted samples. These results attest to the feasibility of HbGp/Nafion/GCE for the quality control of commercial milk samples possibly contaminated with H_2O_2.

Table 2 Analytical recoveries of H_2O_2 added in milk samples, measured by the HbGp/Nafion/GCE biosensor

Sample	H_2O_2 added (μM)	H_2O_2 found (μM)	Recovery (%)
Pure milk	5.96	5.71	95.83
	11.851	12.79	107.84
	25.34	23.30	91.93
Centrifuged milk	7.94	7.71	97.21
	15.75	16.15	102.56
	25.34	25.16	99.29
Diluted milk (10^{-3})	7.94	7.63	96.10
	15.75	16.31	103.56
	25.34	25.09	99.00

Conclusions

Giant extracellular hemoglobin from *Glossoscolex paulistus*, here defined as HbGp, undergoes an oxidation process in the presence of H_2O_2, forming ferryl-HbGp. The same reaction can be studied on the surface of an electrochemical biosensor, as in the case of HbGp/Nafion/GCE proposed in this work, making it possible to detect and quantify low levels of the mentioned oxidizing agent. When building the device, the previous modification of the electrodic support with Nafion was necessary to make the hemoglobin electroactive and offer a biocompatible microenvironment for its immobilization. The oligomeric stability of the macromolecule in the presence of this conducting polymer was confirmed by both voltammetric and spectroscopic tests. The electrochemical reaction between H_2O_2 and HbGp was favored in an acidic medium, becoming faster and limited by diffusion. Operating the biosensor under optimized conditions, it was possible to quantify low levels of H_2O_2 in milk samples with high precision and accuracy. Therefore, HbGp/Nafion/GCE represents a

potential alternative for quality control testing of samples supposedly contaminated by this additive.

Supplementary Information The online version contains supplementary material available at https://doi.org/10.1007/s00216-022-04020-8.

Acknowledgements The authors are grateful to the Chemical Analysis Center of the Federal University of Maranhão, Brazil, for the infrastructure used in the spectroscopic analyses.

Funding The authors received financial assistance granted by the National Council for Scientific and Technological Development (CNPQ; Proc. 420261/2018–4, 407891/2018–8 and 308108/2020–5). Evair D. Nascimento also received scholarship from CAPES.

Declarations

Conflict of interest The authors declare no competing interests.

References

1. Belato FA, Schrago CG, Coates CJ, Halanych KM, Costa-Paiva EM, Eyre-Walker A. Newly discovered occurrences and gene tree of the extracellular globins and linker chains from the giant hexagonal bilayer hemoglobin in metazoans. Genome Biol Evol. 2019;11:597–612. https://doi.org/10.1093/gbe/evz012.
2. Righi G. Notas sobre os oligochaeta glossoscolecidae do Brasil. Arq Zool. 1971;20:1–95.
3. Barros AEB, Caruso CS, Alves FR, Tabak M, Carvalho FAO. Characterization of the apo-form of extracellular hemoglobin of Glossoscolex paulistus (HbGp) and its stability in the presence of urea. Eur Biophys J. 2020;49:449–62. https://doi.org/10.1007/s00249-020-01449-6.
4. Bachega JFR, Maluf FV, Andi B, Pereira HDM, Carazzollea MF, Orville AM, Tabak M, Brandão-Neto J, Garratt RC, Reboredo EH. The structure of the giant haemoglobin from Glossoscolex paulistus. Acta Crystallogr Sect D Biol Crystallogr. 2015;71:1257–71. https://doi.org/10.1107/S1399004715005453.
5. Bachega JFR, Bleicher L, Horjales ER, Santiago PS, Garratt RC, Tabak M. Crystallization and preliminary structural analysis of the giant haemoglobin from Glossoscolex paulistus at 3.2 Å. J Synchrotron Radiat. 2011;18:24–8. https://doi.org/10.1107/S090904951002772X.
6. Royer WE, Knapp JE, Strand K, Heaslet HA. Cooperative hemoglobins: conserved fold, diverse quaternary assemblies and allosteric mechanisms. Trends Biochem Sci. 2001;26:297–304. https://doi.org/10.1016/S0968-0004(01)01811-4.
7. Carvalho FAO, Caruso CS, Nascimento ED, Oliveira TMBF, Bachega JFR, Tabak M. Oligomeric stability of Glossoscolex paulistus hemoglobin as a function of the storage time. Int J Biol Macromol. 2019;133:30–6. https://doi.org/10.1016/j.ijbiomac.2019.04.072.
8. Carvalho FAO, Santiago PS, Borges JC, Tabak M. On the molecular mass of the extracellular hemoglobin of Glossoscolex paulistus: analytical ultracentrifugation reexamination. Anal Biochem. 2009;385:257–63. https://doi.org/10.1016/j.ab.2008.11.008.
9. Moreira LM, Moraes PCG, Mendonça JPRF, Guimarães L, Lyon JP, Aimbire F, Poli AL, Imasato H. Hemoglobina extracelular gigante de glossoscolex paulistus: um extraordinário sistema supramolecular hemoproteico. Quim Nova. 2011;34:119–30.
10. Moreira LM, Poli AL, Lyon JP, Moraes PCG, Mendonça JPRF, Aimbire F, Barbosa VC, Imasato H (2011) Giant extracellular hemoglobin of Glossoscolex paulistus: an excellent prototype of biosensor and blood substitute. Biosens Heal Environ Biosecurity. https://doi.org/10.5772/19008
11. Krajewska A, Radecki J, Radecka H. A voltammetric biosensor based on glassy carbon electrodes modified with single-walled carbon nanotubes/hemoglobin for detection of acrylamide in water extracts from potato crisps. Sensors. 2008;8:5832–44. https://doi.org/10.3390/s8095832.
12. Barros AEB, Carvalho FAO, Alves FR, Carvalho JWP, Tabak M. Denaturant effects on HbGp hemoglobin as monitored by 8-anilino-1-naphtalene-sulfonic acid (ANS) probe. Int J Biol Macromol. 2015;74:327–36. https://doi.org/10.1016/j.ijbiomac.2014.12.035.
13. Carvalho FAO, Alves FR, Carvalho JWP, Tabak M. Guanidine hydrochloride and urea effects upon thermal stability of Glossoscolex paulistus hemoglobin (HbGp). Int J Biol Macromol. 2015;74:18–28. https://doi.org/10.1016/j.ijbiomac.2014.11.012.
14. Carvalho FAO, Carvalho JWP, Alves FR, Tabak M. PH effect upon HbGp oligomeric stability: characterization of the dissociated species by AUC and DLS studies. Int J Biol Macromol. 2013;59:333–41. https://doi.org/10.1016/j.ijbiomac.2013.04.070.
15. Carvalho JWP, Alves FR, Batista T, Carvalho FAO, Santiago PS, Tabak M. Sodium dodecyl sulfate (SDS) effect on the thermal stability of oxy-HbGp: dynamic light scattering (DLS) and small angle X-ray scattering (SAXS) studies. Colloids Surfaces B Biointerfaces. 2013;111:561–70. https://doi.org/10.1016/j.colsurfb.2013.06.050.
16. Carvalho JWP, Carvalho FAO, Santiago PS, Tabak M. Thermal denaturation and aggregation of hemoglobin of Glossoscolex paulistus in acid and neutral media. Int J Biol Macromol. 2013;54:109–18. https://doi.org/10.1016/j.ijbiomac.2012.11.022.
17. Carvalho JWP, Carvalho FAO, Batista T, Santiago PS, Tabak M. Cetyltrimethylammonium chloride (CTAC) effect on the thermal stability of oxy-HbGp: dynamic light scattering (DLS) and small angle X-ray scattering (SAXS) studies. Colloids Surfaces B Biointerfaces. 2014;118:14–24. https://doi.org/10.1016/j.colsurfb.2014.03.021.
18. Oliveira JBS, Ramos L, Souza CO, Sebastião I, Caruso C, Carvalho FAO, Carvalho JWP, Morgante PG, Santiago PS. Initial biophysical characterization of Amynthas gracilis giant extracellular hemoglobin (HbAg). Eur Biophys J. 2020;49:473–84. https://doi.org/10.1007/s00249-020-01455-8.
19. Muzzelo C, Neely C, Shah P, Abdulmalik O, Elmer J. Prolonging the shelf life of Lumbricus terrestris erythrocruorin for use as a novel blood substitute. Artif Cells, Nanomedicine Biotechnol. 2018;46:39–46. https://doi.org/10.1080/21691401.2017.1290645.
20. Polo ÉM, Santos RP, Moreira LM, Yazbeck GM. Bioinformatical development of oligonucleotides for the D chain gene of the giant extracellular hemoglobin of Glossoscolex paulistus. Int J Biosci Biochem Bioinforma. 2014;4:67–70. https://doi.org/10.7763/ijbbb.2014.v4.312.
21. Harnois T, Rousselot M, Rogniaux H, Zal F. High-level production of recombinant Arenicola marina globin chains in Escherichia coli: a new generation of blood substitute. Artif Cells, Blood Substitutes, Biotechnol. 2009;37:106–16. https://doi.org/10.1080/10731190902908445.
22. Weber RE, Vinogradov SN. Nonvertebrate hemoglobins: functions and molecular adaptations. Physiol Rev. 2001;81:569–628. https://doi.org/10.1152/physrev.2001.81.2.569.
23. Rousselot M, Delpy E, La Rochelle CD, Lagente V, Pirow R, Rees JF, Hagege A, Le Guen D, Hourdez S, Zal F. Arenicola marina extracellular hemoglobin: a new promising blood substitute. Biotechnol J. 2006;1:333–45. https://doi.org/10.1002/biot.200500049.
24. Caruso CS, Biazin E, Carvalho FAO, Tabak M, Bachega JFR. Metals content of Glossoscolex paulistus extracellular

hemoglobin: its peroxidase activity and the importance of these ions in the protein stability. J Inorg Biochem. 2016;161:63–72. https://doi.org/10.1016/j.jinorgbio.2016.05.002.
25. Libardi SH, Alves FR, Tabak M. Interaction of Glossoscolex paulistus extracellular hemoglobin with hydrogen peroxide: formation and decay of ferryl-HbGp. Int J Biol Macromol. 2018;111:271–80. https://doi.org/10.1016/j.ijbiomac.2017.12.147.
26. Sun Y, Chen W, Li X, Yu Q, Zhu Y, Wang Y, Chen L, Sun W, Li G, Niu Y (2021) Electrochemical performance and electrocatalytic behavior of myoglobin modified TiO2@3D graphene composite electrode. Int J Electrochem Sci 16:1–9. https://doi.org/10.20964/2021.10.11
27. Murphy M, Theyagarajan K, Thenmozhi K, Senthilkumar S. Direct electrochemistry of covalently immobilized hemoglobin on a naphthylimidazolium butyric acid ionic liquid/MWCNT matrix. Colloids Surfaces B Biointerfaces. 2021;199:111540. https://doi.org/10.1016/j.colsurfb.2020.111540.
28. Yang YJ, Chen S, Wang N, Yang P, Jiang C, Liu M, Cheng Y (2021) The preparation of reduced graphene oxide/hemoglobin/CdS biocomposite and its electrocatalysis for the reduction of hydrogen peroxide. Fullerenes, Nanotub Carbon Nanostructures 1–8 . https://doi.org/10.1080/1536383X.2021.1990268
29. Murphy M, Theyagarajan K, Ganesan P, Senthilkumar S, Thenmozhi K. Electrochemical biosensor for the detection of hydrogen peroxide using cytochrome c covalently immobilized on carboxyl functionalized ionic liquid/multiwalled carbon nanotube hybrid. Appl Surf Sci. 2019;492:718–25. https://doi.org/10.1016/j.apsusc.2019.06.283.
30. Aghamiri ZS, Mohsennia M, Rafiee-Pour HA. Immobilization of cytochrome c on polyaniline/polypyrrole/carboxylated multiwalled carbon nanotube/glassy carbon electrode: biosensor fabrication. J Solid State Electrochem. 2019;23:2233–42. https://doi.org/10.1007/s10008-019-04300-x.
31. Jahanbakhshi M (2018) Myoglobin immobilized on mesoporous carbon foam in a hydrogel (selep) dispersant for voltammetric sensing of hydrogen peroxide. Microchim Acta 185. https://doi.org/10.1007/s00604-017-2654-9
32. Carbone M, Aneggi E, Figueredo F, Susmel S (2022) NiO-nanoflowers decorating a plastic electrode for the non-enzymatic amperometric detection of H2O2 in milk: Old issue, new challenge. Food Control 132. https://doi.org/10.1016/j.foodcont.2021.108549
33. Yan Y, Zhang Z, Xiao M, Zhou H. Anchor of ni2+ on the agmatine sulfate-modified electrodes for the determination of H2O2 in food. Surf Rev Lett. 2017;24:1–8. https://doi.org/10.1142/S0218625X17500081.
34. Kirdar SS, Atamer M. Quality criteria of Tulum cheese produced from cow's milk preserved by activation of lactoperoxidase system. J Food Process Preserv. 2021;45:1–8. https://doi.org/10.1111/jfpp.15210.
35. Arefin S, Sarker MAH, Islam MA, Harun-ur-Rashid M, Islam MN. Use of hydrogen peroxide (H2O2) in raw cow's milk preservation. J Adv Vet Anim Res. 2017;4:371–7. https://doi.org/10.5455/javar.2017.d236.
36. He L, Qian W, Cen L, Shen S, Wang S, Chen S, Liu S, Liu A, Yang Y, Liu Y (2021) Catalase-conjugated collagen surfaces and their application for the quantification determination of H2O2 in milk. Lwt 147. https://doi.org/10.1016/j.lwt.2021.111601
37. Santiago PS, Carvalho FAO, Domingues MM, Carvalho JWP, Santos NC, Tabak M. Isoelectric point determination for Glossoscolex paulistus extracellular hemoglobin: oligomeric stability in acidic pH and relevance to protein-surfactant interactions. Langmuir. 2010;26:9794–801. https://doi.org/10.1021/la100060p.
38. Zuccarello L, Barbosa C, Todorovic S, Silveira CM. Electrocatalysis by heme enzymes—applications in biosensing. Catalysts. 2021;11:218. https://doi.org/10.3390/catal11020218.
39. Peng L, Utesch T, Yarman A, Jeoung JH, Steinborn S, Dobbek H, Mroginski MA, Tanne J, Wollenberger U, Scheller FW. Surface-tuned electron transfer and electrocatalysis of hexameric tyrosine-coordinated heme protein. Chem - A Eur J. 2015;21:7596–602. https://doi.org/10.1002/chem.201405932.
40. Pereira AR, Sedenho GC, de Souza JCP, Crespilho FN. Advances in enzyme bioelectrochemistry. An Acad Bras Cienc. 2018;90:825–57. https://doi.org/10.1590/0001-3765201820170514.
41. Gorton L, Lindgren A, Larsson T, Munteanu FD, Ruzgas T, Gazaryan I. Direct electron transfer between heme-containing enzymes and electrodes as basis for third generation biosensors. Anal Chim Acta. 1999;400:91–108. https://doi.org/10.1016/S0003-2670(99)00610-8.
42. Abrantes-Coutinho VE., Santos AO, Moura RB, Pereira-Junior, FN. Mascaro LH, Morais S, Oliveira TMBF (2021) Systematic review on lectin-based electrochemical biosensors for clinically relevant carbohydrates and glycoconjugates. Colloids and Surfaces B: Biointerfaces. 208 . https://doi.org/10.1016/j.colsurfb.2021.112148
43. Naresh V, Lee N. A review on biosensors and recent development of nanostructured materials-enabled biosensors. Sensors (Switzerland). 2021;21:1–35. https://doi.org/10.3390/s21041109.
44. Roche J, Royer CA (2018) Lessons from pressure denaturation of proteins. J R Soc Interface 15. https://doi.org/10.1098/rsif.2018.0244
45. Samajdar RN, Manogaran D, Yashonath S, Bhattacharyya AJ. Using porphyrin-amino acid pairs to model the electrochemistry of heme proteins: experimental and theoretical investigations. Phys Chem Chem Phys. 2018;20:10018–29. https://doi.org/10.1039/c8cp00605a.
46. Sana Rafiq H, Fatima B, Hussain D, Mohyuddin A, Majeed S, Manzoor S, Imran M, Nawaz R, Shabbir S, Mukhtar S, Naeem Ashiq M, Najam-ul-Haq M. Selective electrochemical sensing of hemoglobin from blood of β-thalassemia major patients by tellurium nanowires-graphene oxide modified electrode. Chem Eng J. 2021;419:129706. https://doi.org/10.1016/j.cej.2021.129706.
47. de Oliveira GA, Gevaerd A, Blaskievicz SF, Zarbin AJG, Orth ES, Bergamini MF, Marcolino-Junior LH. A simple enzymeless approach for Paraoxon determination using imidazole-functionalized carbon nanotubes. Mater Sci Eng C. 2020;116:111140. https://doi.org/10.1016/j.msec.2020.111140.
48. Rasouli H, Naji L, Hosseini MG. The influence of electrodeposited PPy film morphology on the electrochemical characteristics of Nafion-based energy storage devices. J Electroanal Chem. 2019;836:165–75. https://doi.org/10.1016/j.jelechem.2019.02.007.
49. Blanco PM, Madurga S, Garcés JL, Mas F, Dias RS. Influence of macromolecular crowding on the charge regulation of intrinsically disordered proteins. Soft Matter. 2021;17:655–69. https://doi.org/10.1039/d0sm01475c.
50. Murtaugh ML, Fanning SW, Sharma TM, Terry AM, Horn JR. A combinatorial histidine scanning library approach to engineer highly pH-dependent protein switches. Protein Sci. 2011;20:1619–31. https://doi.org/10.1002/pro.696.
51. Yang AS, Honig B. On the pH dependence of protein stability. J Mol Biol. 1993;231:459–74.
52. Santiago PS, Moura F, Moreira LM, Domingues MM, Santos NC, Tabak M. Dynamic light scattering and optical absorption spectroscopy study of pH and temperature stabilities of the extracellular hemoglobin of Glossoscolex paulistus. Biophys J. 2008;94:2228–40. https://doi.org/10.1529/biophysj.107.116780.
53. Moreira LM, Santiago PS, de Almeida ÉV, Tabak M. Interaction of giant extracellular Glossoscolex paulistus hemoglobin (HbGp) with zwitterionic surfactant N-hexadecyl-N, N-dimethyl-3-ammonio-1-propanesulfonate (HPS): effects of oligomeric dissociation.

Colloids Surfaces B Biointerfaces. 2008;61:153–63. https://doi.org/10.1016/j.colsurfb.2007.07.010.
54. Su Y, Zhou X, Long Y, Li W (2018) Immobilization of horseradish peroxidase on amino-functionalized carbon dots for the sensitive detection of hydrogen peroxide. Microchim Acta 185. https://doi.org/10.1007/s00604-017-2629-x
55. Liu H, Gao J, Duan C, Wu K, Guo K. A novel mediator-free biosensor based on hemoglobin immobilized in the Au nanoparticals and TiO2 nanosheets co-modified graphene nanocomposite. Mater Lett. 2020;275:128142. https://doi.org/10.1016/j.matlet.2020.128142.
56. Xu W, Sakran M, Fei J, Li X, Weng C, Yang W, Zhu G, Zhu W, Zhou X. Electrochemical biosensor based on HRP/Ti3C2/Nafion film for determination of hydrogen peroxide in serum samples of patients with acute myocardial infarction. ACS Biomater Sci Eng. 2021;7:2767–73. https://doi.org/10.1021/acsbiomaterials.1c00242.
57. Elancheziyan M, Senthilkumar S. Covalent immobilization and enhanced electrical wiring of hemoglobin using gold nanoparticles encapsulated PAMAM dendrimer for electrochemical sensing of hydrogen peroxide. Appl Surf Sci. 2019;495:143540. https://doi.org/10.1016/j.apsusc.2019.143540.
58. Huang H, Lv L, Chen Z, Chen Y, Hu Y, Xu F. Dysprosium oxide-graphene oxide supported hemoglobin for biosensing of H2O2. Chem Lett. 2019;48:114–7. https://doi.org/10.1246/cl.180782.
59. He F, Qin X, Bu L, Fu Y, Tan Y, Chen C, Li Y, Xie Q, Yao S. Study on the bioelectrochemistry of a horseradish peroxidase-gold nanoclusters bionanocomposite. J Electroanal Chem. 2017;792:39–45. https://doi.org/10.1016/j.jelechem.2017.03.033.
60. Chen G, Sun H, Hou S. Electrochemistry and electrocatalysis of myoglobin immobilized in sulfonated graphene oxide and Nafion films. Anal Biochem. 2016;502:43–9. https://doi.org/10.1016/j.ab.2016.03.003.
61. Chao J, Zou M, Zhang C, Sun H, Pan D, Pei H, Su S, Yuwen L, Fan C, Wang L. A MoS2-based system for efficient immobilization of hemoglobin and biosensing applications. Nanotechnology. 2015;26:274005. https://doi.org/10.1088/0957-4484/26/27/274005.
62. Gabunada JC, Vinothkannan M, Kim DH, Kim AR, Yoo DJ. Magnetite nanorods stabilized by polyaniline/reduced graphene oxide as a sensing platform for selective and sensitive non-enzymatic hydrogen peroxide detection. Electroanalysis. 2019;31:1–1. https://doi.org/10.1002/elan.201900134.
63. Han L, Cui S, Deng D, Li Y, Yan X, He H, Luo L. Synthesis of Ag-Au/reduced graphene oxide/TiO2 nanocomposites: application as a non-enzymatic amperometric H2O2 sensor. Curr Anal Chem. 2020;16:485–92. https://doi.org/10.2174/1573411015666181126103804.
64. Zhang H, Zhang Y, Liu S. Preparation of trace Fe2P modified N, P Co-doped carbon materials and their application to hydrogen peroxide detection. Electroanalysis. 2020;32:1–8. https://doi.org/10.1002/elan.202060445.